AIP | Journal of Applied Physics

Enhanced cryogenic magnetocaloric effect in Eu8Ga16Ge30 clathrate nanocrystals

Anis Biswas, Sayan Chandra, Stevce Stefanoski, J. S. Blázquez, J. J. Ipus, A. Conde, M. H. Phan, V. Franco, G. S. Nolas, and H. Srikanth

Citation: Journal of Applied Physics **117**, 033903 (2015); doi: 10.1063/1.4906280
View online: http://dx.doi.org/10.1063/1.4906280
View Table of Contents: http://scitation.aip.org/content/aip/journal/jap/117/3?ver=pdfcov
Published by the AIP Publishing

Enhanced cryogenic magnetocaloric effect in $Eu_8Ga_{16}Ge_{30}$ clathrate nanocrystals

Anis Biswas,[1,a),b)] Sayan Chandra,[1,c)] Stevce Stefanoski,[1,d)] J. S. Blázquez,[2] J. J. Ipus,[2] A. Conde,[2] M. H. Phan,[1] V. Franco,[2] G. S. Nolas,[1] and H. Srikanth[1,b)]
[1]*Department of Physics, University of South Florida, Tampa, Florida 33620, USA*
[2]*Dpto. Física de Materia Condensada, ICMSE-CSIC, Universidad de Sevilla, Sevilla 41080, Spain*

(Received 10 November 2014; accepted 8 January 2015; published online 20 January 2015)

We observe an enhanced magnetic entropy change ($-\Delta S_M$) at cryogenic temperatures ($T < 20\,K$) in $Eu_8Ga_{16}Ge_{30}$ clathrate (type-I) nanocrystals prepared by a ball milling method. With reduction in the crystal size to 15 nm, $-\Delta S_M$ is enhanced at low temperatures, reaching the highest value ($\sim$10 J/kg K) at 5 K for a field change of 5 T. For all samples investigated, there is a cross-over temperature ($\sim$25 K) in $-\Delta S_M$ (T) above which $-\Delta S_M$ decreases with crystal size, opposite to that observed at low temperatures. A careful analysis of the magnetic and magnetocaloric data reveals that as the crystal size decreases the magnetic interaction between Eu^{2+} ions on the Eu2 site governing the primary ferromagnetic transition at $\sim$35 K becomes gradually weaker, in effect, altering the interaction between Eu^{2+} ions occupying the Eu1 and Eu2 sites responsible for the secondary ferromagnetic transition at 15 K. As a result, we have observed a strong change in magnetization and the enhancement of $-\Delta S_M$ at low temperature. © *2015 AIP Publishing LLC*.
[http://dx.doi.org/10.1063/1.4906280]

INTRODUCTION

The magnetocaloric effect (MCE) in magnetic materials is of topical interest for its possible applications in magnetic refrigeration.[1–6] One major emphasis for the research in this area is to find refrigerant materials exhibiting a large MCE in different temperature regimes, from room temperature to cryogenic temperatures. Two distinct temperature ranges of practical interests are near room temperature and below liquid nitrogen temperature (the so-called cryogenic temperature range).[1] Among the known magnetocaloric materials, Gd and $GdSi_2Ge_2$ are considered to be prospective candidates for refrigeration near room temperature. On the other hand, several compounds and intermetallic alloys, such as Ho_5Pd_2, $DyAl_2$, $HoCo_2$, $ErCo_2$, HoNiSi, $HoRu_2Si_2$, and $GdPO_4$, have been reported to show large MCE at low temperature and are therefore promising for cryogenic magnetic refrigeration.[1–5] It should be noted that these intermetallic alloys possess a relatively low resistivity, thus causing huge eddy current losses when used in actual magnetic cooling devices. Some also exhibit considerable thermal and magnetic hysteresis losses which are undesirable for active magnetic refrigeration.[7] Current research is therefore focused on investigating refrigerant materials that not only show large MCE but also possess high resistivity and negligible hysteresis losses.[8,9]

Clathrate compounds continue to attract interest in the research community owing to their desirable thermoelectric and magnetic properties.[10–19] Generally in clathrates, one or more "guest" atoms of one kind reside inside a "host" framework structure formed by other species. In the case of $Eu_8Ga_{16}Ge_{30}$, the interstitial sites are fully occupied by Eu.[14–17] There exist two different crystal structures with this composition, type-I and type-VIII.[15] In the unit cell of the type-I clathrate Eu resides inside two different polyhedra, two inside pentagonal dodecahedra centered at the 2*a* crystallographic site (Eu1) and six inside hexagonal tetrakaidecahedra centered at the 6*d* crystallographic site (Eu2). On the other hand, eight distorted pentagonal dodecahedra containing 23 vertices surround Eu^{2+} ions in the case of the type-VIII clathrate.[15,19] The ferromagnetism in these clathrates is attributed to the indirect Ruderman-Kittel-Kasuya-Yoshida (RKKY) interaction between Eu^{2+} ions.[14–19] In the case of the type-I $Eu_8Ga_{16}Ge_{30}$, a paramagnetic (PM) to ferromagnetic (FM) transition is observed at $T_C \sim 35\,K$ followed by a second magnetic transition at $T_L \sim 15\,K$.[19] The transitions at T_C and T_L are hereafter denoted as the first and second transitions, respectively. It has been argued that the magnetic interaction between Eu^{2+} ions at the Eu2 sites mainly gives rise to the first transition, whereas the second transition results from the magnetic interaction between Eu^{2+} ions occupying Eu1 and Eu2 sites. The presence of these two successive transitions resulted in the enhanced magnetocaloric response of this material.[19] Previous studies focused mainly on bulk properties of type-I $Eu_8Ga_{16}Ge_{30}$,[11–19] however an investigation into the effect of reducing the crystal size to nanometer scale on the magnetic and magnetocaloric properties of this material has not been reported.

In this article, we report a large reversible cryogenic MCE (below 20 K) in $Eu_8Ga_{16}Ge_{30}$ clathrate (type-I) nanocrystals prepared by ball milling. While single phase ferromagnetic materials show a decrease in $-\Delta S_M$ with

[a)]Present address: Ames Laboratory, Iowa State University, Ames, Iowa 50011, USA.
[b)]Authors to whom correspondence should be addressed. Electronic addresses: anisbiswas@ameslab.gov and sharihar@usf.edu
[c)]Present address: ÉNERGIE MATÉRIAUX TÉLÉCOMMUNICATIONS, INRS, Québec J3X 1S2, Canada.
[d)]Present address: Geophysical Laboratory, Carnegie Institution of Washington, Washington, DC 20015, USA.

decreasing the crystal size in general, we observe an enhancement of $-\Delta S_M$ with decreasing crystal size at low temperatures in this material. The sample with the largest average crystal size (~42 nm) shows a table-like MCE[20,21] over a relatively wide temperature range.

SAMPLE PREPARATION AND CHARACTERIZATION

The type-I $Eu_8Ga_{16}Ge_{30}$ nanocrystals were prepared in two steps. First, high quality polycrystalline $Eu_8Ga_{16}Ge_{30}$ was synthesized following the method discussed previously.[19] Next, the obtained materials were ball milled in an Argon atmosphere for different lengths of times to obtain samples with different crystallite sizes. Milling was carried out at 200 rpm in Argon atmosphere in a *Fritsch Pulverisette Vario 4* using Si_3N_4 bowls and balls as milling media, with a ball to powder mass ratio of 10. We denote the three sets of samples ball milled for 2.5, 5, and 10 h as S1, S2, and S3, respectively. Ball milling for over 10 h produced only amorphous materials. X-ray diffraction (XRD) and energy dispersive spectroscopy (EDS) measurements on the prepared samples confirmed the crystallite type-I clathrate phase without oxygen impurity. For XRD study, Cu-Kα radiation was used. The XRD patterns of the samples are shown in Fig. 1. The average crystallite size was determined from the XRD patterns using the Scherrer's formula[22] and from transmission electron microscopy (TEM). As shown in Fig. 1, the peaks in the XRD pattern gradually broaden with increasing ball milling time, an indication of the reduction in crystallite size with increasing ball milling time. From the Scherrer's formula, the calculated average crystallite sizes for the three samples S1, S2, and S3 are 42 (±6), 34 (±8), and 15 (±7) nm, respectively. All results are in good agreement with those calculated from the TEM micrographs. As an example, a typical TEM image for S3 is shown in inset of Fig. 1. We note that an amorphous phase exists in each sample, which is evidenced by noisy data of XRD pattern. To quantify the amount of the amorphous phase, the XRD patterns of samples were fitted by TOPAS 4.2 software using two phases: a crystalline clathrate phase and an amorphous phase. For crystalline phase, we take the lattice parameter of bulk (unmilled) sample (a= 10.690 Å; Pm-3n space group). We have found that the fraction of amorphous phase increases with the ball milling time. It is about 33%, 58%, and 70% for S1, S2, and S3, respectively. However, there is hardly any change in lattice parameter of crystalline phase in the samples.

EXPERIMENTAL RESULTS AND DISCUSSION

A physical property measurement system from Quantum Design equipped with a vibrating sample magnetometer (VSM) probe was used for magnetic characterization. The temperature dependence of the field cooled magnetization, M (T), measured in a temperature range of 5–70 K in the presence of a 0.2 T magnetic field is shown in Fig. 2. There exist clear signatures of the first and second transitions at $T_C \sim 35$ K and $T_L \sim 15$ K in the M (T) curves for all samples. The transition temperature is assigned as the inflection point of dM/dT vs. T plots. As a representative example, the dM/dT vs. T curve for S1 is shown in the inset of Fig. 2. The observed T_C and T_L agree well with those of bulk polycrystalline $Eu_8Ga_{16}Ge_{30}$ (type-I).[19] In order to investigate the magnetocaloric properties of the ball milled samples, we have calculated $-\Delta S_M$ from the isothermal magnetic field (H) dependence of magnetization curves following Maxwell's relation:[1]

$$\left[\frac{\partial S(T,H)}{\partial H}\right]_T = \left[\frac{\partial M(T,H)}{\partial T}\right]_H.$$

The temperature dependence of $-\Delta S_M$ for 0.2 T and 5 T magnetic field changes for the three samples are shown in Figs. 3(a) and 3(b). As seen in these figures, all samples exhibit large $-\Delta S_M$ at low temperatures (below ~20 K) while $-\Delta S_M$ gradually increases with decreasing particle size. For S3, $-\Delta S_M$ reaches a value of ~10 J/kg K for a field change of 5 T at the lowest temperature (~5 K). This value of $-\Delta S_M$ is comparable to those of the so-called giant magnetocaloric materials at low temperatures reported in the literature.[1]

In general, the presence of disordered grain boundaries (GB) plays an important role in the magnetic properties of fine particle systems.[23–26] Typically, crystalline defects or

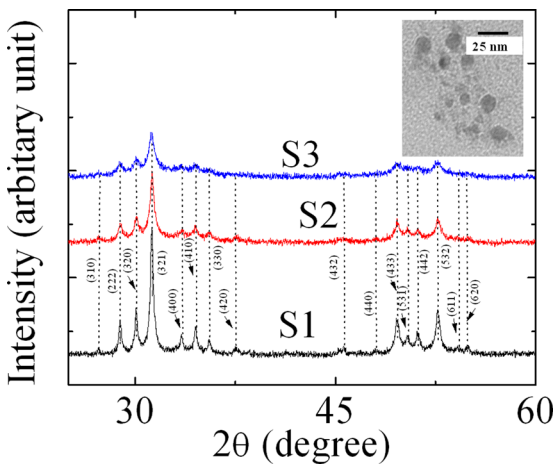

FIG. 1. XRD patterns of the three clathrate samples prepared for this study. Inset: A typical TEM image of sample S3.

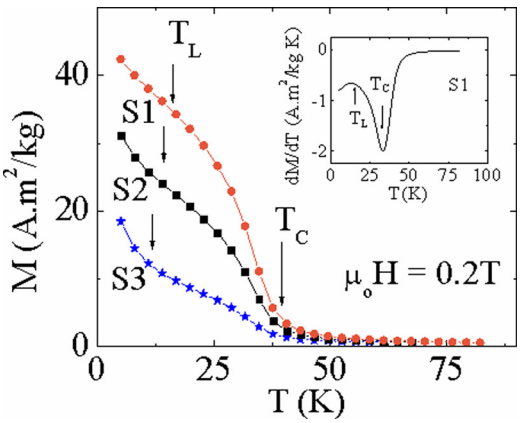

FIG. 2. The temperature dependence of field cooled magnetization taken in a field of 0.2 T for the $Eu_8Ga_{16}Ge_{30}$ clathrates. The transition temperatures T_C and T_L for the samples are indicated by arrows. Inset: the dM/dT vs. T plot for S1.

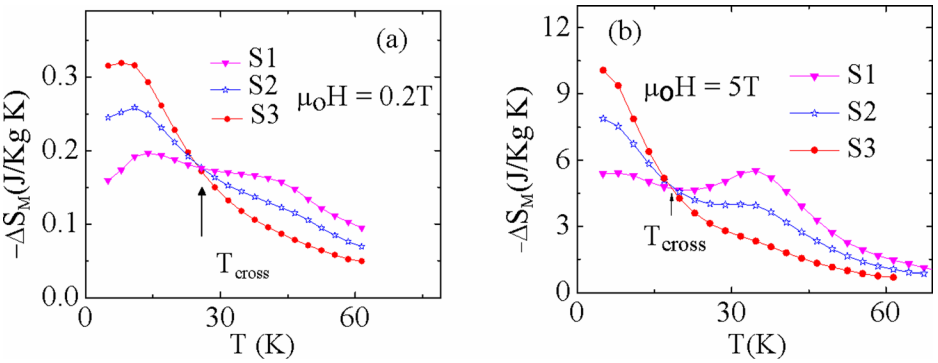

FIG. 3. The temperature dependence of the magnetic entropy change for the samples for magnetic field changes of (a) 0.2 T and (b) 5 T. The cross-over temperature (T_{cross}) is denoted by an arrow.

dislocations exist near GB regions which effectively decreases the value of $-\Delta S_M$.[26] In this context, our finding of an enhancement in $-\Delta S_M$ at low temperatures with decreasing crystallite size is unique. In the case of fine particles, it has been suggested that the ordering of surface spins can contribute to $-\Delta S_M$.[27] The effect of surface spins is mostly realized at low temperatures and increases as the particle size of a material decreases. One might therefore attribute this to the enhancement of $-\Delta S_M$ observed at low temperatures in the present case. However, we have observed the enhancement of $-\Delta S_M$ in an applied magnetic field as low as 0.2 T, a magnetic field that is often insufficient to align the magnetic moments of disordering surface spins.[28] Moreover, the alignment of surface spins in high magnetic fields cannot be solely the cause for the observed large $-\Delta S_M$ ($\sim$10 J/kg K) obtained in our sample. The MCE at low temperatures for these clathrate-nanocrystals, therefore, must be associated with the intrinsic magnetic transitions of the system. Apart from this, we observed that the $-\Delta S_M$ (T) for the samples dramatically changes above a certain cross-over temperature ($T_{cross} \sim 25$ K). In the temperature region above T_{cross}, $-\Delta S_M$ decreases with decreasing crystallite size. For all three samples, T_{cross} remains almost the same irrespective of the applied magnetic field. The existence of a nearly constant T_{cross}, for all samples, indicates that the observed enhancement in $-\Delta S_M$ at low temperature should not be associated with ordering of surface spins alone. Otherwise, T_{cross} should change from sample to sample as the relative fraction of surface spins varies depending on their mean crystallite size. In addition, the temperature at which the effect of surface spins is pronounced for each sample also depends on the applied magnetic field. Hence, T_{cross} should have a strong magnetic field dependence, in contrast with our observation.

A question may arise regarding the significance of T_{cross}. As discussed earlier, the bulk $Eu_8Ga_{16}Ge_{30}$ (type-I) sample with micron-sized grains possesses two magnetic transitions at T_C and T_L.[19] Our recent magnetocaloric study on this system has pointed out the existence of two peaks in $-\Delta S_M$(T) due to these transitions;[19] however, the maximum value of $-\Delta S_M$ (ΔS_{max}) at T_C is considerably larger than that at T_L. This clearly indicates that the first transition has a dominant contribution to the MCE in the material in bulk form.[19] Since the M (T) data of the ball milled samples show two magnetic transitions at T_C and T_L, similar to that of the bulk, it is reasonable to infer that the MCE of the particle systems are also governed by these transitions. To quantify their influence on $-\Delta S_M$ (T), we define a parameter $R(=\frac{d\Delta S_M}{dT})$ which represents the rate of change in ΔS_M with T. For all samples investigated herein, R(T) shows two maxima at $\sim T_C$ and $\sim T_L$, as the largest magnetic entropy changes occur near the transitions (Fig. 4). Depending on the impact of a transition on ΔS_M, the peak values of the maxima

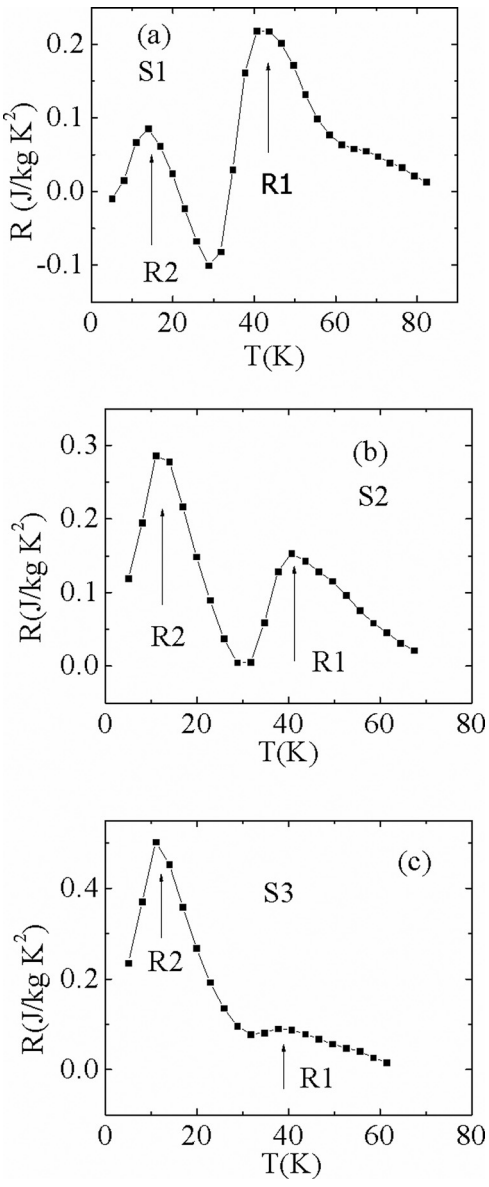

FIG. 4. R vs. T plots for (a) S1, (b) S2, and (c) S3. Here, R is calculated from the ΔS_M (T) data at 5 T.

will change. We denote the peak values of R (T) at T_C and T_L as R_1 and R_2, respectively, and define ΔR as $\Delta R = (R_2 - R_1)$. For S1, R_1 is slightly larger than R_2, whereas R_2 exceeds R_1 for the other two samples. The values of R_2 and ΔR increase with decreasing crystallite size, while R_1 consistently decreases with decreasing crystallite size. From the behavior of R (T), two inferences can be made. First, the second transition (at $\sim T_L$) has a greater influence on the MCE of the ball milled samples than the first transition, unlike the case of the bulk sample. Second, the effect of the second transition on MCE is strengthened with decreasing crystallite size, as is reflected in the systematic increase of R_2 and ΔR from sample S1 to S3. As a consequence, there is an enhancement of $-\Delta S_M$ at low temperature with decreasing crystallite size. The decrease of R_1 with decreasing crystallite size indicates that the impact of the first transition on MCE gradually diminishes from larger to smaller crystallite sizes. It should be noted that the peak in $-\Delta S_M$ (T) at $\sim T_L$ for S1 becomes comparable to that due to the transition at $\sim T_C$. The presence of two broad maxima with nearly equal peak values gives rise to a table-like $-\Delta S_M$ (T) observed for this sample.[20,21] Thus, from the foregoing discussion, it is clear that the MCE at low temperatures is intrinsically related to the second transition. As an increase of $-\Delta S_M$ with decreasing crystallite size is observed below T_{cross} in both high and low magnetic fields, we conclude that the onset of the second transition occurs below T_{cross} ($\sim T_L$) for all three samples. The crystallite size dependence of $-\Delta S_M$ above and below T_{cross} is therefore completely different. With decreasing crystallite size, the impact of the second transition on the MCE becomes stronger giving rise to a larger $-\Delta S_M$.

Now let us discuss the possible reasons behind the gradual increase of the impact of the transition at low temperature on the MCE in these samples. We constructed Arrott plots (M^2 vs. $\mu_o H/M$ data) for all the three samples (Figs. 5(a)–5(c)). The positive intercept on the M^2 axis from the extrapolation of high field data implies the presence of spontaneous magnetization (M_{sp}) in the system 5(a)–5(c).[29] The temperature at which M_{sp} starts to develop is denoted as T_{sp}. From the Arrott plots, it is clear that for S_1 M_{sp} develops just below T_C (defined from derivative of M vs. T curve as shown in Fig. 2), i.e., $T_{sp} \sim T_C$, however T_{sp} gradually shifts to lower temperature with T_C for the other two samples. In particular, for S3 M_{sp} develops only below 15 K. Generally, for a ferromagnetic system the M_{sp} develops simultaneously with the occurrence of a ferromagnetic transition, hence, T_{sp} coincides with T_C. One might have a question regarding the occurrence of a ferromagnetic transition at T_C ($\sim$35 K) for S3. We have measured M (T) in the zero-field-cooled (ZFC), field cooled cooling (FCC), and field cooled warming (FCW) protocols for all the samples. The ZFC and field cooled curves for S3 (inset in Fig. 5(c)) show a clear bifurcation below $\sim$30 K, similar to samples S1 and S2. Such a bifurcation cannot be possible without stabilization of any magnetic correlation in the sample.[30] Based on these observations, we conclude that for all three samples the ferromagnetic transition occurs at $T_C \sim 35$ K. However, with the reduction in crystallite size, the ferromagnetic ordering is significantly suppressed. Since grain boundaries are the origins of non-

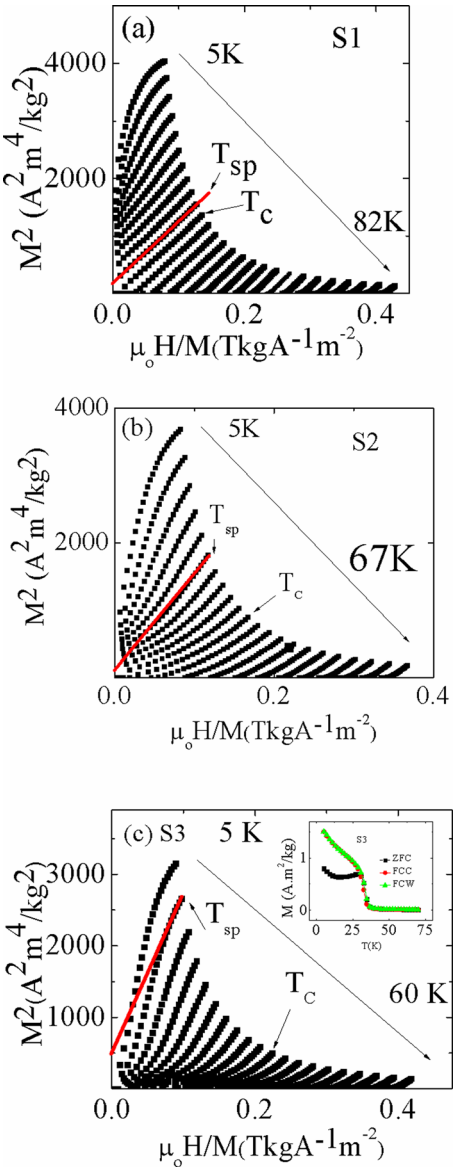

FIG. 5. Arrott plots for S1, S2, and S3 are shown in (a), (b) and (c), respectively. The T_C values are determined from derivative of the M (T) curves, as shown in Fig. 2. The temperature dependence of M measured in the presence of a field of 0.05 T in the ZFC, FCC, and FCW protocols for S3 is shown in the inset of (c).

crystallinity, crystalline disorders, and/or dislocations, they can affect the ferromagnetic correlation in the samples. Moreover, the presence of an amorphous phase in the grain boundary region might also have an effect. The increase of the fraction of a non-crystalline phase with ball milling, as observed from the XRD analysis, is an indication of the increasing fraction of non-crystalline grain boundaries with decreasing crystallite size. As a result, the ferromagnetic ordering due to the transition at T_C becomes gradually disrupted with decreasing crystallite size, indicating a gradual shift to a temperature associated with the development of M_{SP} with respect to T_C. On the other hand, the transition at low temperature is a secondary ferromagnetic transition occurring in a pre-existing ferromagnetic state. If that pre-existing ferromagnetic state is disrupted because of grain boundary effects, the relative change in M due to the secondary transition becomes more prominent. An increase in the

relative change in M can enhance $-\Delta S_M$, as observed in our clathrate samples.

The large magnetic entropy changes observed at low temperature in these fine clathrate particles indicates their potential for cryogenic magnetic refrigeration. Since the MCE can also be tuned by varying the particle size, their use will provide more flexibility in practical applications. In $Eu_8Ga_{16}Ge_{30}$, the ferromagnetism is attributed to the RKKY interaction,[19] which is nearly isotropic[31] and would not drive any significant anisotropic MCE effect for this material. This aspect of $Eu_8Ga_{16}Ge_{30}$ is highly desirable for cooling applications.[1]

SUMMARY

In summary, type-I $Eu_8Ga_{16}Ge_{30}$ clathrate nanocrystals have been successfully prepared by ball milling and exhibit a large and tunable cryogenic MCE below ~20 K. In contrast to bulk $Eu_8Ga_{16}Ge_{30}$, the MCE at low temperatures is predominantly governed by the magnetic transition at T_L, which in bulk samples, arises due to the indirect RKKY interaction between Eu^{2+} ions occupying Eu1 and Eu2 sites in the system. Interestingly, $-\Delta S_M$ at low temperatures increases with decreasing crystallite size, with the largest value (10 J/kg K at 5 K) for a field change of 5 T obtained for the sample with the smallest average crystal size (~15 nm). There exists a cross-over temperature T_{cross} above which an opposite trend is observed. The sample with the largest average crystallite size (~37 nm) shows a table-like $-\Delta S_M$ (T) desirable for active magnetic refrigeration.

ACKNOWLEDGMENTS

A.B., S.C., M.H.P., and H.S. thank the U.S. Department of Energy, Office of Basic Energy Sciences, Division of Materials Sciences and Engineering under Award No. DE-FG02-07ER46438 (magnetic measurements and analysis). S.S. and G.S.N. acknowledge the support of the U.S. Department of Energy, Basic Energy Sciences, Division of Materials Science and Engineering under Award No. DE-FG02-04ER46145 for bulk synthesis of polycrystalline $Eu_8Ga_{16}Ge_{30.}$ The work at Sevilla University was supported by the Spanish MINECO and EU FEDER (Project MAT 2013-45165-P) and the PAI of the Regional Government of Andalucía (Project P10-FQM-6462) for the synthesis of nanocrystalline Eu8Ga16Ge30.

[1]K. A. Gschneidner, Jr., V. K. Pecharsky, and A. O. Tsokol, Rep. Prog. Phys. **68**, 1479 (2005).
[2]T. Samanta, I. Das, and S. Banerjee, Appl. Phys. Lett. **91**, 082511 (2007).
[3]H. Zhang, Y. Y. Wu, Y. Long, H. Wang, K. Zhong, F. Hu, J. Sun, and B. Shen, J. Appl. Phys. **116**, 213902 (2014).
[4]T. Paramanik, K. Das, T. Samanta, and I. Das, J. Appl. Phys. **115**, 083914 (2014).
[5]E. Palacios, J. A. Rodríguez-Velamazán, M. Evangelisti, G. J. McIntyre, G. Lorusso, D. Visser, L. J. de Jongh, and L. A. Boatner, Phys. Rev. B **90**, 214423 (2014).
[6]V. Franco, J. S. Blazquez, B. Ingale, and A. Conde, Annu. Rev. Mater. Res. **42**, 305 (2012).
[7]A. Giguere, M. Foldeaki, B. Ravi Gopal, R. Chahine, T. K. Bose, A. Frydman, and J. A. Barclay, Phys. Rev. Lett. **83**, 2262 (1999).
[8]A. Biswas, T. Samanta, S. Banerjee, and I. Das, Appl. Phys. Lett. **91**, 013107 (2007).
[9]M. H. Phan and S. C. Yu, J. Magn. Magn. Mater. **308**, 325 (2007).
[10]G. S. Nolas, G. A. Slack, and S. B. Schujman, in *Semiconductors and Semimetals*, edited by T. M. Tritt (Academic Press, New York, 2001), Vol. 69, p. 255.
[11]G. S. Nolas, J. L. Cohn, G. A. Slack, and S. B. Schujman, Appl. Phys. Lett. **73**, 178 (1998).
[12]J. Martin, H. Wang, and G. S. Nolas, Appl. Phys. Lett. **92**, 222110 (2008).
[13]Y. Sasaki, K. Kishimoto, T. Koyanagi, H. Asada, and K. Akai, J. Appl. Phys. **105**, 073702 (2009).
[14]B. C. Sales, B. C. Chakoumakos, R. Jin, J. R. Thompson, and D. Mandrus, Phys. Rev. B **63**, 245113 (2001).
[15]S. Paschen, W. Carrillo-Cabera, A. Bentien, V. H. Tran, M. Baenitz, Y. Grin, and F. Steglich, Phys. Rev. B **64**, 214404 (2001).
[16]G. T. Woods, J. Martin, M. Beekman, R. P. Hermann, F. Grandjean, V. Keppens, O. Leupold, G. J. Long, and G. S. Nolas, Phys. Rev. B **73**, 174403 (2006).
[17]M. H. Phan, G. T. Woods, A. Chaturvedi, S. Stefanoski, G. S. Nolas, and H. Srikanth, Appl. Phys. Lett. **93**, 252505 (2008).
[18]*The Physics and Chemistry of Inorganic Clathrates*, edited by G. S. Nolas (Springer, 2014).
[19]M. H. Phan, V. Franco, A. Chaturvedi, S. Stefanoski, G. S. Nolas, and H. Srikanth, Phys. Rev. B **84**, 054436 (2011).
[20]A. Biswas, T. Samanta, S. Banerjee, and I. Das, J. Appl. Phys. **103**, 013912 (2008).
[21]A. Chaturvedi, S. Stefanoski, M. H. Phan, G. S. Nolas, and H. Srikanth, Appl. Phys. Lett. **99**, 162513 (2011).
[22]A. J. C. Wilson, Proc. Phys. Soc. London **80**, 286 (1962).
[23]R. H. Kodama, A. E. Berkowitz, E. J. McNiff, and S. Foner, Phys. Rev. Lett. **77**, 394 (1996).
[24]J. M. D. Coey, Phys. Rev. Lett. **27**, 1140 (1971).
[25]A. Biswas, I. Das, and C. Majumdar, J. Appl. Phys. **98**, 124310 (2005).
[26]A. Biswas, S. Chandra, M. H. Phan, and H. Srikanth, J. Alloys Compd. **545**, 157 (2012).
[27]P. Poddar, S. Srinath, J. Gass, B. L. V. Prasad, and H. Srikanth, J. Phys. Chem. C **111**, 14060 (2007).
[28]S. Chandra, H. Khurshid, W. Li, G. C. Hadjipanayis, M. H. Phan, and H. Srikanth, Phys. Rev. B **86**, 014426 (2012).
[29]A. K. Pramanik and A. Banerjee, Phys. Rev. B **82**, 094402 (2010).
[30]R. Mathieu, P. Nordblad, D. N. H. Nam, N. H. Phuc, and N. V. Khiem, Phys. Rev. B **63**, 174405 (2001).
[31]P. N. Patrone and T. L. Einstein, Phys. Rev. B **85**, 045429 (2012).